# Packing Effects in the Liquid-Phase Adsorption of $C_5$–$C_{22}$ *n*-Alkanes on ZSM-5

**Kurt M. A. De Meyer,[†] Shaji Chempath,[‡] Joeri F. M. Denayer,*[,†] Johan A. Martens,[§] Randall Q. Snurr,[‡] and Gino V. Baron[†]**

*Department of Chemical Engineering, Vrije Universiteit Brussel, Pleinlaan 2, B-1050 Brussel, Belgium, Department of Chemical Engineering, 2145 Sheridan Road, Northwestern University, Evanston, Illinois 60208, and Center for Surface Science and Catalysis, Katholieke Universiteit Leuven, Kasteelpark Arenberg 23, B-3001 Leuven, Belgium*

*Received: May 22, 2003; In Final Form: July 23, 2003*

The liquid-phase adsorption of $C_5$–$C_{22}$ linear alkanes on ZSM-5 was studied using a batch adsorption technique. Saturation capacities of the alkanes depend strongly on the chain length. The number of $-CH_x$ groups adsorbed per unit cell drops steeply between $C_7$ and $C_8$ and then increases steadily to reach a plateau of 53−54 for $C_{14}$−$C_{22}$. In this plateau region, the pores of ZSM-5 are densely packed with alkane molecules. The mechanisms of packing in liquid-phase adsorption were studied using configurational-bias grand canonical Monte Carlo simulations. These simulations revealed that the probability of bending and crossing in the intersections increases with chain length, explaining the very good packing of long-chain alkanes. Short alkanes tend to stay away from the intersections, resulting in a lower packing density.

## Introduction

Zeolite pores are of molecular size and offer a selective environment for catalytic and separative processes. The description of molecular packing in these pores is not straightforward but certainly relevant to the understanding of zeolite functioning. It is often found that saturation capacities, expressed in volume adsorbed per zeolite mass unit, depend on the size of the molecule,[1−4] as expected for adsorption in a restrained geometry. Generally, smaller molecules are able to pack more efficiently and have access to areas in the zeolite that are inaccessible to larger molecules. Besides, the organization of molecules in the pores depends on the architecture of the pore system. In one-dimensional pores of narrow size, pore filling can be achieved by nose to tail arrangement of molecules. For materials with intersecting pore systems, it can be suspected that parts of the structure are inaccessible as a result of blocking of intersections by long or bulky molecules. A typical example of a zeolite with intersecting pores is ZSM-5. This zeolite has a two-dimensional pore structure consisting of straight channels (pore size, 0.51 × 0.55 nm) with intersecting sinusoidal channels (pore size, 0.54 × 0.56 nm),[5] composed of 10-membered oxygen rings (Figure 1). Each unit cell is constructed from four segments of linear channel, four segments of sinusoidal channel, and four channel intersections.

Many research groups have studied the adsorption of alkanes of different size on ZSM-5. Adsorption isotherms of specific *n*- and isoalkanes deviate from the usual Langmuir type and contain a kink at compound-specific partial pressures,[1,3,6] and an inflection point in the adsorption enthalpy and entropy versus zeolite loading curves.[7,8] The two-step behavior of these linear and branched alkanes is usually interpreted in terms of the ZSM-5 channel geometry (vide infra). Preferential adsorption of molecules in sinusoidal and/or linear channels or even in the intersections and a strong dependence of these adsorption mechanisms on temperature, pressure, and zeolite loading have been found in experimental studies.[1,2,6,8−15] The confinement of alkanes in the ZSM-5 pore system has also been investigated by computational molecular modeling techniques. Configurational-bias Monte Carlo simulations showed that the underlying mechanism of the occurrence of a kink in the adsorption isotherms of $C_6$ and $C_7$ on ZSM-5 originates from a "commensurate freezing" of molecules in the sinusoidal channels.[16] Other simulations focused on the distribution of alkanes in the

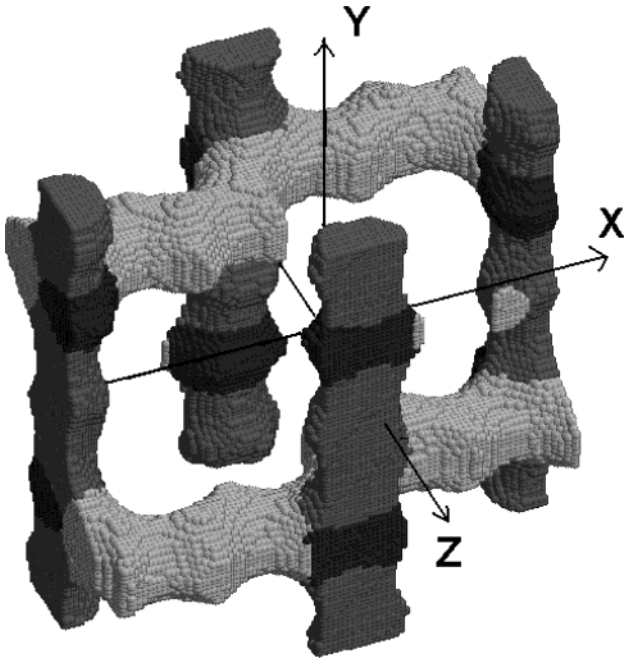


**Figure 1.** Schematic representation of the H−ZSM-5 channel structure: straight channels (dark gray) run in the *y* direction; zigzag channels (light gray) run in the *x* direction. Intersections are shown with black spheres.

* Corresponding author. E-mail: Joeri.denayer@vub.ac.be.
[†] Vrije Universiteit Brussel.
[‡] Northwestern University.
[§] Katholieke Universiteit Leuven.

10.1021/jp0354144 CCC: $25.00 
Published on Web 09/10/2003

**TABLE 1: Literature Data of Adsorption Capacities, in Molecules Per Unit Cell, of *n*-Alkanes on H−ZSM-5**

| CN 1 | CN 2 | CN 3 | CN 4 | CN 5 | CN 6 | CN 7 | CN 8 | CN 9 | CN 10 | ref. |
|---|---|---|---|---|---|---|---|---|---|---|
| 17.0 | 15.1 | 12.7 | 10.3 | | | | | | | 27 |
| 8.7 | 13.2 | 11.7 | 9.8 | | | | | | | 9 |
| 7.2 | 10.7 | 9.8 | 8.2 | | | | | | | 6 |
| 16.2 | 12.5 | 11.5 | 10.0 | | | | | | | 28 |
| | 15.0 | 12.0 | 10.0 | 8.5 | 8.0 | 7.0 | | | | 25 |
| | 10.6 | 10.7 | 9.3 | | 7.9 | | | | | 1 |
| | | 13.1 | 10.9 | 9.9 | 7.9 | 6.9 | 5.9 | 3.8 | 3.1 | 10 |
| | | | 8.0 | 8.0 | 8.1 | 7.9 | 5.0 | | | 8 |
| | | | 9.3 | 8.7 | 8.1 | 7.3 | 5.4 | 5.1 | 5.1 | 19 |
| | | | | 8.5 | 8.4 | 7.4 | 5.2 | 5.2 | 4.9 | 3 |
| | | | | 8.5 | 8.0 | 7.0 | | | | 29 |
| | | | | | 8.2 | | | | 3.8 | 8 |
| | | | | | 7.9 | | | | | 20 |

different channels as a function of temperature, pressure, zeolite loading, and alkane chain length.[17,18]

Saturation adsorption capacities of $C_1$–$C_{10}$ *n*-alkanes have been determined by various techniques and are summarized here in Table 1. Generally, it is found that the adsorption capacity, expressed in molecules adsorbed per unit cell, decreases with carbon number. A steep drop in adsorption capacity is observed between $C_6$ and $C_8$.[2,3,19] The most probable explanation for this less efficient packing of $C_7$ and $C_8$ molecules compared to shorter ones is that $C_6$ molecules fit nicely within the sinusoidal channel segment, while longer molecules protrude into the intersections and thus partially obstruct filling of adjacent sections.[16] No attention has been paid in the literature to the packing of long-chain alkanes. However, it is expected that packing of molecules with lengths that are up to three times larger than that of the pore segments requires a high degree of organization. In the present work, adsorption capacities of $C_5$–$C_{22}$ *n*-alkanes in ZSM-5 were determined experimentally. Configurational-bias grand canonical Monte Carlo simulations of the liquid-phase adsorption of $C_5$–$C_{14}$ *n*-alkanes were also performed to understand the underlying adsorption mechanisms. An analysis has been made in terms of packing efficiency, molecule flexibility or ability to bend, and crossover of molecules in the intersections.

## Experimental Section

The experiments were performed with H−ZSM-5, obtained by de-ammoniating an $NH_4$−ZSM-5 zeolite obtained from Zeolyst (CBV 8014, $SiO_2/Al_2O_3$ mole ratio of 80) in a muffle oven in the presence of air. Temperature programming was the following: at 1 K/min from 303 to 383 K, 1 h at 383 K, then at 1 K/min from 383 to 523 K, 1 h at 523 K, and finally at 1 K/min from 523 to 673 K. This final temperature was kept during 40 h.

Sorption uptake measurements were obtained by means of batch experiments. Zeolite samples (~1 g) were put in 10 mL glass vials. After regeneration (1 K/min from 303 to 383 K, 1 h at 383 K, then at 1 K/min from 383 to 673 K, 24 h at 673 K), the vials were immediately (at 673 K) sealed with a cap with a septum in order to avoid the uptake of water and other components from the air and were weighed to determine the regenerated zeolite mass. A mixture of a linear alkane in a nonadsorbing solvent was prepared. All hydrocarbons used were of high-purity grade (≥99%) from Merck and Acros. In most experiments, iso-$C_8$ (99.5% purity, Acros) was used as nonadsorbing solvent.[20] A comparative experiment with tri-isopropylbenzene, a much more bulky molecule, as solvent gave exactly the same adsorption capacities, confirming the nonadsorbing character of iso-$C_8$.

Immediately after sealing the cap and weighing the sample, about 10 mL of the mixture was injected through the septum into the zeolite-containing vials, and another 10 mL was added to a vial without zeolite, to be used as blank sample. Samples were kept at 277 K, to be sure no compounds could evaporate, and stirred frequently.

In all measurements, liquid samples were taken after 24 and 48 h, to verify if equilibrium between adsorbed and bulk phase was achieved, and analyzed in a gas chromatograph with flame ionization detector.

The GC was equipped with an HP-5 column (5%/95% diphenyl-/dimethylsiloxane copolymer), with a length of 30 m, film thickness of 0.25 $\mu$m, and internal diameter of 320 $\mu$m. The temperature programming of the GC oven was dependent on the mixtures used. For each sample (zeolite and blank), three GC analyses were performed and the average was used in further calculations. Calibration lines, obtained from other experiments,[21] were used to guarantee a high precision in the calculation of the amounts adsorbed. For each sample the amount adsorbed ($q_{sorbate}$) at equilibrium was obtained by calculation of the mass balance:

$$q_{sorbate} = \left( \frac{(wt\%_{blank} - wt\%_{zeolite})(m^0_{sorbate} + m^0_{solvent})}{100 m_{zeolite}} \right) \quad (1)$$

with $m^0$ the initial mass added to the zeolite-containing recipient and $m_{zeolite}$ the regenerated zeolite mass.

To obtain accurate adsorption measurements, the total concentration of the adsorbing component was about 0.20 mL/g zeolite. No change in amounts adsorbed was observed for four times higher concentrations, indicating that the plateau in the adsorption isotherm was always reached.

**Simulation Details.** All simulations were done using the configurational bias grand canonical Monte Carlo (CB-GCMC) technique and treating the methyl ($CH_3$) and methylene ($CH_2$) groups as united atoms. Only the adsorbed phase is simulated with specified fugacity, volume, and temperature as in a typical GCMC simulation. Simulations were done in 8 unit cells of silicalite at 300 K. The fugacity of the linear alkane corresponding to the liquid-phase composition was calculated using the Peng−Robinson equation of state assuming the gas-phase is ideal. iso-$C_8$ was not simulated because it is nonadsorbing as proved in the Experimental Section. The force field parameters used here have been previously optimized for vapor−liquid equilibrium of alkanes[22] and alkane adsorption in silicalite.[23] A more detailed explanation of the methodology and the parameters are given in ref 24. To obtain convergence of adsorption data, 4−10 million Monte Carlo steps were used for simulations of $C_5$ to $C_{12}$ and 60 million steps were used for simulation of $C_{14}$.

## Results and Discussion

**Experimental Results.** Figure 2 shows the uptake of pure $C_6$, $C_8$, $C_{10}$, and $C_{16}$ in H−ZSM-5 from iso-$C_8$. The adsorbed amounts remain constant after 30 min, indicating that the experiments were performed under equilibrium conditions. Even after 4 days equilibration time, the amounts adsorbed did not alter at all. The saturation capacities of all tested *n*-alkanes, expressed in the number of molecules adsorbed per unit cell (UC) and total number of carbon atoms per unit cell, are given in Figure 3. At equilibrium, $C_5$ and $C_6$ adsorb about 7.6 molecules/(ZSM-5 unit cell). From $C_6$ to $C_8$, a sudden drop in the number of molecules adsorbed per unit cell is observed ($C_5$, 7.6 molecules/UC; $C_6$, 7.6 molecules/UC; $C_7$, 6.6 molecules/

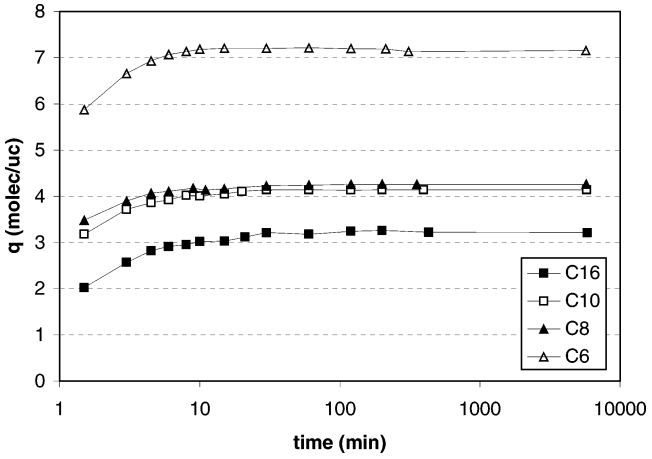


**Figure 2.** Uptake of $C_6$, $C_8$, $C_{10}$, and $C_{16}$ from iso-$C_8$ on H−ZSM-5 as a function of time.

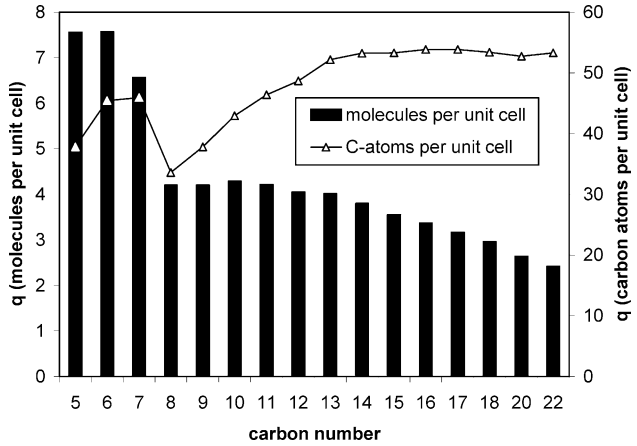


**Figure 3.** Adsorption capacities of $C_5$–$C_{22}$ *n*-alkanes in H−ZSM-5 expressed in molecules per unit cell and number of $-CH_x$ groups adsorbed per unit cell.

UC; $C_8$, 4.2 molecules/UC). A similar observation was found in other studies (see Table 1). From $C_8$ on, the number of molecules adsorbed per unit cell decreases gradually, to reach a value of 2.5 molecules/UC for $C_{22}$.

A more interesting picture is obtained when the number of $-CH_x$ groups is plotted as a function of the carbon number (Figure 3). For $C_5$, a unit cell contains 38 $-CH_x$ groups, and for $C_6$ and $C_7$ 45 $-CH_x$ groups are adsorbed per unit cell, while, for $C_8$, only 34 $-CH_x$ groups are adsorbed per unit cell. From $C_8$ on, the number of $-CH_x$ groups per unit cell increases steadily, to reach a maximum of about 53−54 $-CH_x$ groups per unit cell from $C_{14}$ on. For molecules shorter than $C_{14}$, it appears that the available space in the pores of ZSM-5 is thus not completely used, and gaps must be present between the adsorbed molecules.

**Alkane Siting According to Molecular Modeling.** The dependence of adsorption capacity on chain length should be attributed to the organization and siting of *n*-alkanes in the ZSM-5 channel system. To gain a better understanding of the molecular details, the adsorption of $C_5$ to $C_{14}$ *n*-alkanes from liquid phase, which leads to high zeolite loading, was studied using CB-GCMC calculations. Table 2 gives the calculated zeolite loading at 300 K obtained for a mixture of 98 mol % iso-$C_8$ and 2 mol % of the adsorbing alkane. The calculated capacities correspond very well with the experimental ones except for the case of $C_{14}$, where the simulations clearly underestimate the real capacity.

The packing efficiency is seen to be a function of the alkane chain length. $C_5$ and $C_6$ have lengths less than the distance between intersections, and occupy the channel space between two intersections as shown in Figure 4. $C_7$ crosses the intersection and extends into adjacent channel space, which leads to a lower capacity. $C_8$ and longer alkanes sit in a different way in the pore system. These molecules place the center of their chain near the intersections, with their head and tail dangling into the channels, as is shown in Figure 5 for $C_8$.

In addition to the zeolite−guest interactions, the adsorption patterns are also affected by the intramolecular interactions within the alkane molecule. The torsion angle of each C−C bond has a minimum energy when it is in the trans (anti-) conformation. Thus, based on intramolecular energies, the most stable form of alkanes is their linear, all-trans conformation that also fits well in the straight channels. To fit in the sinusoidal channels, molecules have to bend, by changing torsion angles from anti to gauche, which is energetically less favorable (for the potential model used in the simulations, each anti to gauche transformation costs 3 kJ/mol).

From the simulations, it appears that alkane molecules do not always reside just in one channel type, but that a molecule may start in, e.g., a linear channel segment and end in a sinusoidal channel segment. This kind of molecule bending requires more torsion angles becoming gauche from anti. Table 3 gives the percentage molecules that are bent in this way as a function of the chain length. Whereas short molecules such as $C_5$, $C_6$, and $C_7$ are nearly all in linear conformation, residing either in a straight or a sinusoidal channel, the probability that a molecule resides in two channel types increases rapidly from $C_8$ on. With $C_{14}$, 50% of the molecules bend at the intersection with their head in one channel type and tail in another. Molecule bending in the low-occupancy adsorption of $C_4$ to $C_{25}$ *n*-alkanes on ZSM-5 was studied by Maginn et al. using configurational-bias GCMC.[17] They found that the probability of molecule bending at low coverage and temperature increases from $C_6$ to $C_{12}$ and decreases from $C_{12}$ to $C_{20}$ because, from $C_8$ on, chains became more localized in the straight channels. Residing entirely in the straight channels allows a molecule to maintain close contact with the pore walls, keeping a nearly all-trans conformation. However, for adsorption from liquid phase, we find that the zeolite pores are almost full, and both type of channels (sinusoidal and straight) are occupied by the alkanes. Snapshots of the liquid-phase adsorption of $C_{14}$ are given in Figure 6. Clearly, the pores of silicalite are crowded with $C_{14}$ molecules (bottom snapshot of Figure 6). In the top snapshot, it can be seen how a $C_{14}$ molecule starts in a sinusoidal channel and bends in the intersection to end in a straight channel. Remarkably, the middle snapshot shows how two $C_{14}$ molecules cross each other at the intersection. Although this crossing of molecules at the intersections occurs rarely according to the simulations (<5%), it can shed light on the very high experimental packing efficiency obtained with molecules longer than $C_{13}$ (Figure 3). In Figure 7, showing adsorption of $C_{10}$ in silicalite, it can be seen that intersections can in fact be considered as part of the straight channels and that molecules in the sinusoidal channels are not completely obstructing the intersection region. This allows a crossing to occur, as shown in Figure 6. Thus, even though it is not favored both energetically and entropically, a few molecules do cross each other at the intersections.

A quantitative estimation of the crossing events in the intersections of the channel was done by calculating the radial distribution functions (Table 4). Fractions of molecules that come within 5.0 Å of the central atom of the other molecules

**TABLE 2: Comparison of Experimental and Simulated Adsorption Capacities of $C_5$–$C_{22}$ *n*-Alkanes on H−ZSM-5**

| | | capacity | | | | | |
|---|---|---|---|---|---|---|---|
| solute | CN | expt (mL/g) | expt (mmol/g) | expt (molecules/UC) | expt (C atoms/UC) | simulation (C atoms/UC) | adsorbate length[a] (Å) |
| $C_5$ | 5 | 0.14 | 1.25 | 7.56 | 37.8 | 39.8 | 8.84 |
| $C_6$ | 6 | 0.16 | 1.25 | 7.58 | 45.5 | 46.7 | 10.11 |
| $C_7$ | 7 | 0.16 | 1.08 | 6.56 | 45.9 | 41.9 | 11.38 |
| $C_8$ | 8 | 0.11 | 0.69 | 4.20 | 33.6 | 32.1 | 12.65 |
| $C_9$ | 9 | 0.12 | 0.69 | 4.20 | 37.8 | 37.6 | 13.91 |
| $C_{10}$ | 10 | 0.14 | 0.71 | 4.29 | 42.9 | 41.8 | 15.18 |
| $C_{11}$ | 11 | 0.15 | 0.70 | 4.22 | 46.4 | | 16.45 |
| $C_{12}$ | 12 | 0.15 | 0.67 | 4.06 | 48.7 | 47.8 | 17.72 |
| $C_{13}$ | 13 | 0.16 | 0.66 | 4.01 | 52.2 | | 18.99 |
| $C_{14}$ | 14 | 0.16 | 0.63 | 3.80 | 53.2 | 49.0 | 20.25 |
| $C_{15}$ | 15 | 0.17 | 0.59 | 3.56 | 53.3 | | 21.52 |
| $C_{16}$ | 16 | 0.17 | 0.56 | 3.37 | 53.9 | | 22.79 |
| $C_{17}$ | 17 | 0.16 | 0.52 | 3.17 | 53.8 | | 24.06 |
| $C_{18}$ | 18 | 0.16 | 0.49 | 2.97 | 53.4 | | 25.33 |
| $C_{20}$ | 20 | 0.16 | 0.44 | 2.64 | 52.7 | | 27.86 |
| $C_{22}$ | 22 | 0.16 | 0.40 | 2.42 | 53.3 | | 30.40 |

[a] Calculated according to eq 2.

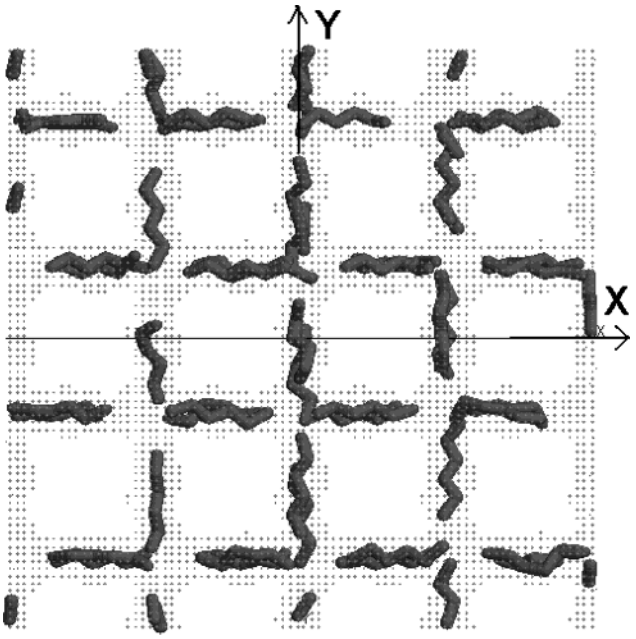


**Figure 4.** Snapshot of $C_6$ molecules in silicalite. The dots represent available pore space.

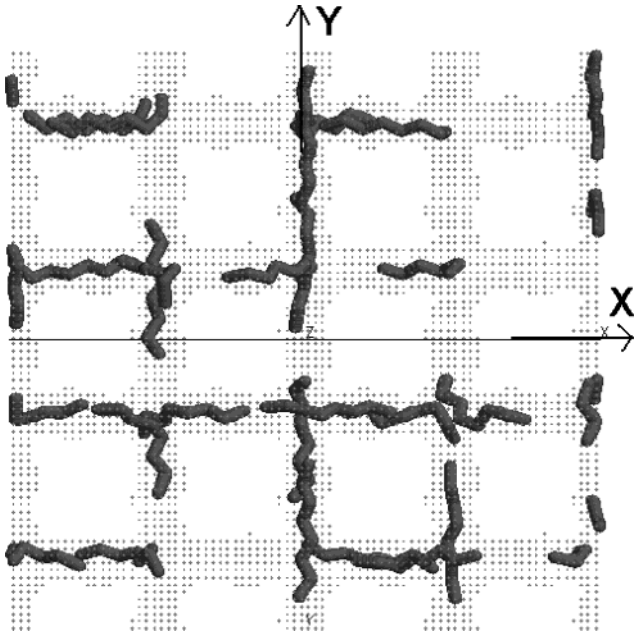


**Figure 5.** Snapshot of $C_8$ molecules in silicalite.

were calculated. These numbers were found to be zero for all *n*-alkanes below $C_8$, 0.67% for $C_8$, 10.5% for $C_{10}$, 12.5% for $C_{12}$, and 15.5% for $C_{14}$. This suggests that the probability of crossing in general increases with length.

From the snapshots it was observed that short molecules will tend to stay away from the intersections and certainly not cross. Complete filling of the pores is not reached in these conditions. Longer alkanes are much more flexible in the pores of ZSM-5, as they bend frequently from one channel type to another. This higher degree of flexibility reduces the probability of blocking of the channel system. Furthermore, the simulations show that with longer chains, the probability to crossover in the intersections increases. Obviously, this feature increases to a large extent the ease with which molecules can efficiently pack in the two-dimensional pore system of ZSM-5.

**Packing Mechanisms.** Experimentally, it is found that, from $C_{14}$ to $C_{22}$, the number of $-CH_x$ groups adsorbed per unit cell remains at a constant value of 53−54. Some older studies report adsorption capacities of 51−52 $-CH_x$ groups adsorbed per unit cell for $C_7$ [3,19] and for $C_{10}$,[19] obtained with gas-phase adsorption measurements. A particular study reports a value of even 55.3 $-CH_x$ groups adsorbed per unit cell for $C_7$.[8] However, most of the data from literature on $C_1$–$C_{10}$ alkanes report lower values for the saturation capacity and certainly no plateau as obtained in the present study for higher alkanes. CB-GCMC simulations of the adsorption of $C_1$–$C_9$ alkanes on silicalite-1 at high pressure give a maximum number of approximately 48 $-CH_x$ groups adsorbed per unit cell of for $C_6$ and $C_7$.[23] Our simulations underestimate the adsorption capacity of $C_{14}$, suggesting that even more crossing of molecules in the intersections may occur than observed from simulations. Chains longer than $C_{14}$ could not be studied by simulations with the current method, because it is very difficult to equilibrate simulations of longer alkanes at high loading.

**TABLE 3: Percentage of Molecules Starting in One Channel Type and Ending in Another**

| molecule | % bent molecules | molecule | % bent molecules |
|---|---|---|---|
| $C_5$ | 1 | $C_9$ | 25 |
| $C_6$ | 1 | $C_{10}$ | 27 |
| $C_7$ | 4 | $C_{12}$ | 45 |
| $C_8$ | 24 | $C_{14}$ | 50 |

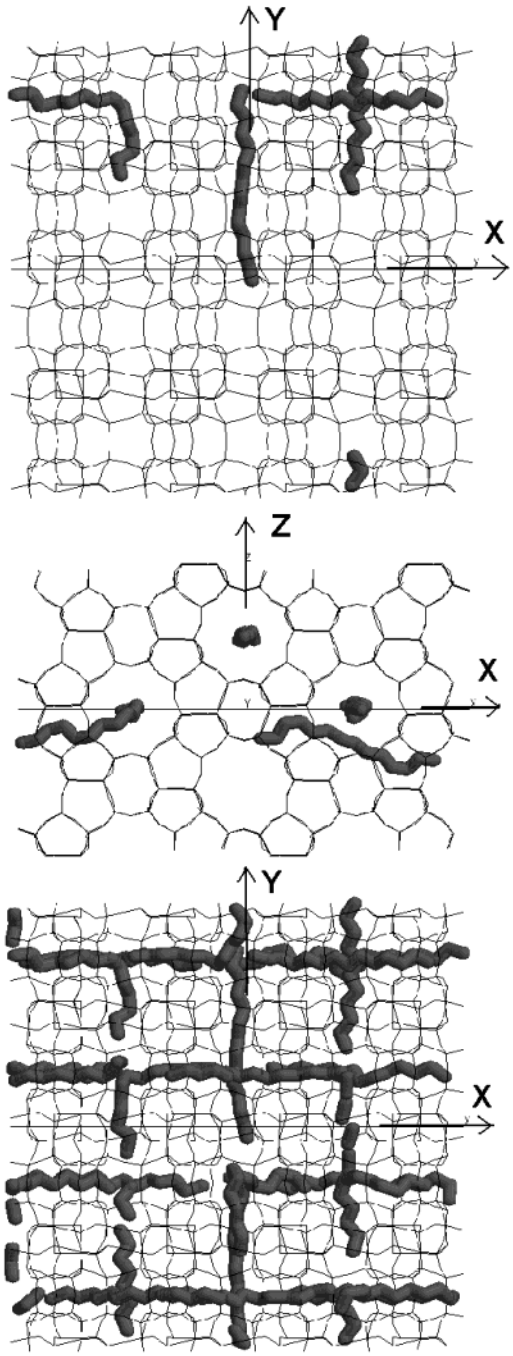


**Figure 6.** Snapshots of $C_{14}$ adsorption in silicalite: (top) View along the *z* axis (four molecules were selected from a snapshot that had 26 $C_{14}$ molecules); (middle) view along the *y* axis (note that the molecules cross at the intersection); (bottom) snapshot of all adsorbed molecules.

The crucial question thus is whether the pores are completely filled with alkanes of these chain lengths or, if in this plateau region, still gaps are present in the adsorbed phase. Attempts have been made in the past to elucidate the mechanisms of adsorption of short alkanes on the basis of dimensions of molecules and channel segments.[1,2,6,9−15] This approach should give an idea of how "filled" the pores really are. Each ZSM-5 unit cell consists of four linear and sinusoidal channel segments and four channel intersections. The length of the straight channel plus intersection is basically the length of a unit cell in the *y* direction (20 Å) divided by 2. The length of the sinusoidal channel plus intersection was estimated to be 11.5 Å. So the total channel length per unit cells equals 86 Å ((4 × 10) + (4 × 11.5) = 86 Å). In this reasoning, the intersections are counted twice, implying that molecules cross each other in the intersections. If the intersections are counted only once, a total length of about 64 Å/(unit cell) is found. Different values for the lengths of *n*-alkane molecules were found in the literature dealing with adsorption in ZSM-5.[1,3,17] In our calculations, we used the following properties to calculate the dimensions of *n*-alkane molecules: C−C lengths of 1.53 Å, H−C lengths of 1.113 Å, C−C−C angles of 114°, and H−C−C angles of 110°. The Lennard-Jones diameter of methyl groups[26] is 3.77 Å, and this forbids neighboring $-CH_x$ groups from becoming closer than 3.77 Å. If nose to tail arrangement of alkanes in the zeolite pores is assumed, the length occupied per individual molecule (expressed in angstroms) can then be calculated as

$$L_i = 1.268(N - 1) + 3.77 \qquad (2)$$

where *N* is the number of carbon atoms in the *n*-alkane molecule. The total occupied lengths of the adsorbed *n*-alkane molecule calculated this way are given in Table 2 and represented graphically in Figure 8. According to this calculation, the highest "adsorbed length" is obtained with $C_{14}$, and equals 77.0 Å/(unit cell). Almost the same value is found for $C_6$. Beyond $C_{14}$, the "adsorbed length" decreases moderately with carbon number, although the number of adsorbed $-CH_x$ groups remains nearly constant ($C_{22}$, 73.6 Å/UC). This total adsorbed length of 77 Å is between the available pore length with the intersections counted twice (86 Å) or only once (64 Å). This would mean there is still free space available for adsorption. Consequently, a chain length dependency of the number of $-CH_x$ groups adsorbed per UC might still be expected, which is observably not the case (Figure 3). In the foregoing reasoning, it is assumed that alkane molecules are separated from each other, as a result of repulsion forces, by a distance of 3.77 Å.

In another empirical length calculation, the number of adsorbed $-CH_x$ groups per unit cell minus one was multiplied with the bond length (corrected for the bond angle). This gives a plateau value of about 66 Å, which corresponds, remarkably enough, quite well to the total length of linear channels, sinusoidal channels, and intersections per UC (64 Å).

To conclude, it appears that the length occupied by the adsorbed molecules is less than the total available length if the intersections are counted twice, but higher than the total available length if the intersections are counted once. This means that molecules with a length larger than that of one channel segment plus intersection necessarily have to cross at the intersections. If not, part of the zeolite pores would be inaccessible as a result of blocking of passages, which would lead to lower values for the "occupied adsorbate length". Crossing at the intersections can occur in various ways. First, alkanes can have their two ends in the same channel type and cross each other as shown in Figure 6 for $C_{14}$. With this kind of crossing, the intersection should indeed be counted twice, as shown schematically in Figure 9. Second, molecules that cross can have their two ends in different channel types (Figure 10). In this case, the number of $-CH_x$ groups is the same as compared to the case in which no crossing occurs, as no overlapping occurs. Further, it remains intriguing that if the additional distance between adsorbed alkane molecules due to intermolecular repulsions is neglected, a length very close to the available length in the pores of ZSM-5 with the intersection counted once is obtained. Although this observation might be a coincidence, it could point at an arrangement of alkanes in which the spatial organization of the alkanes allows tails and heads of long-chain alkanes to approach closely.

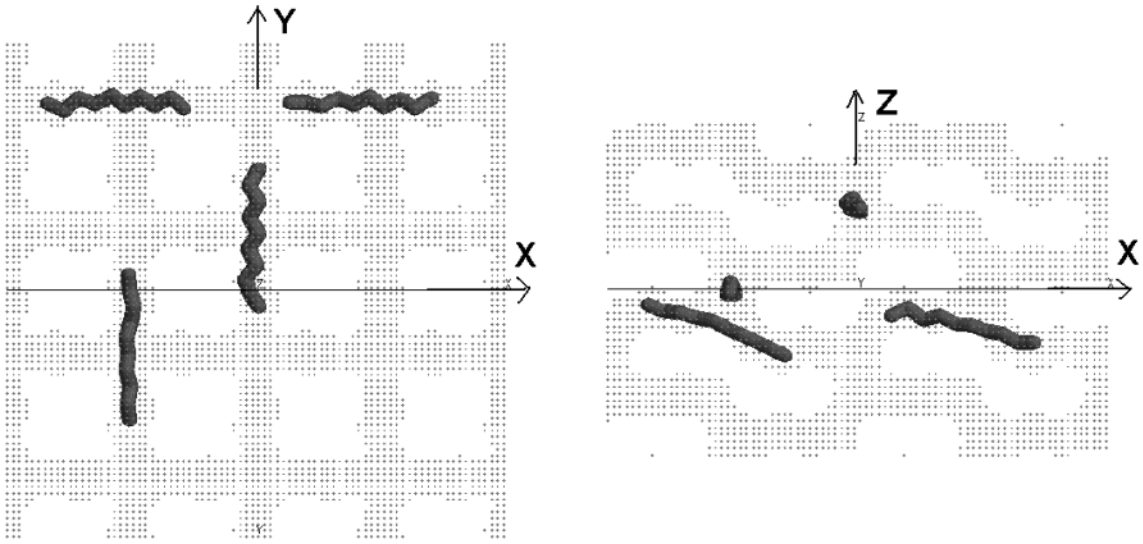


**Figure 7.** Top and side views of $C_{10}$ adsorption in silicalite (four molecules shown here were taken from a snapshot of the CB-GCMC simulation). The dark molecules represent $C_{10}$ in the channels. The dots represent the available pore space.

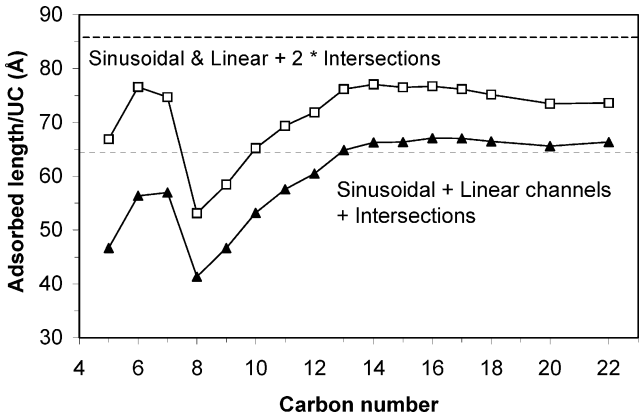


**Figure 8.** Length occupied by *n*-alkanes in the pores of H−ZSM-5 (triangles, length calculation without additional length for repulsion between alkanes; squares, intermolecular repulsion taken into account).

**TABLE 4: Percentage of Molecules Involved in a Crossing/ Passing Event Defined as the Percentage of Molecules That Come to within 5 Å of Another Molecule's Central Atom**

| molecule | % crossover | molecule | % crossover |
|---|---|---|---|
| $C_5$ | 0 | $C_{10}$ | 10.5 |
| $C_6$ | 0 | $C_{12}$ | 12.5 |
| $C_7$ | 0 | $C_{14}$ | 15.5 |
| $C_8$ | 0.67 | | |

On the basis of the above-mentioned arguments, we propose a mechanism in which long chains ($>C_{13}$) are able to cross in the intersections, but preferably in a way such that both ends of the chain are in a different channel type. Shorter molecules are less flexible and give less efficient packing in the pores.

## Conclusions

The adsorption of $C_{5-}C_{22}$ *n*-alkanes in H−ZSM-5 was studied in liquid phase by performing batch sorption uptake experiments. Molecular simulations of alkane adsorption in liquid phase on silicalite-1 were also performed to study siting of the adsorbed molecules. The obtained data provided insight into the dependence of saturation capacity on alkane chain length and the geometry of the pore system and the underlying adsorption mechanisms. $C_5$ and $C_6$ have lengths less than the distance between intersections and avoid sitting in the intersections. $C_7$ crosses the intersection and spans into adjacent channel space, which leads to a lower number of molecules adsorbed per unit

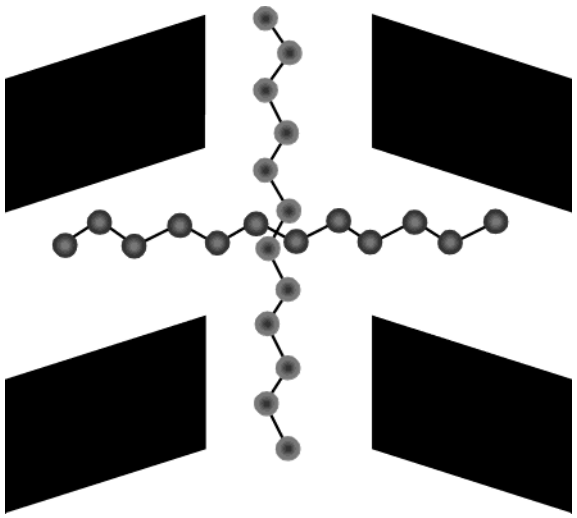

**Figure 9.** Schematic representation of alkane crossing with overlap in the intersection of ZSM-5.

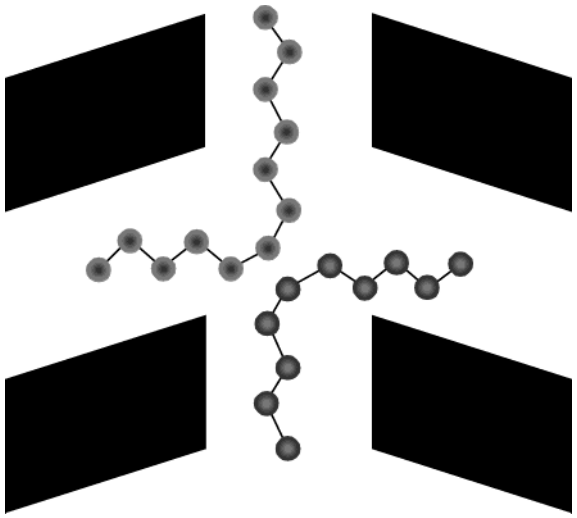

**Figure 10.** Schematic representation of alkane crossing without overlap in the intersection of ZSM-5.

cell. $C_8$ and longer alkanes sit in a different way in the pore system. These molecules place the center of their chain near the intersections, with their head and tail pointing into the channels. This results in a completely different, less efficient type of packing as molecules such as $C_8$ nearly do not bend and do not cross at all in the intersections. With increasing chain length, the probability of bending from one channel type to another and of crossing of alkane molecules in the intersections becomes larger. Accordingly, the number of adsorbed $-CH_x$ groups per UC increases from $C_8$ on until it reaches a plateau for $C_{14-}C_{22}$ of 53−54. The observation that the number of adsorbed $-CH_x$ groups per UC remains constant from $C_{14}$ on indicates that the pore system of ZSM-5 is completely and very densely packed.

**Acknowledgment.** This research was financially supported by FWO Vlaanderen (Grant 0127.99). R.Q.S. and S.C. thank the U.S. National Science Foundation for financial support. J.F.M.D. is grateful to FWO Vlaanderen, for a fellowship as a postdoctoral researcher. The involved teams are participating in the IAP-PAI programme on Supramolecular Chemistry and Catalysis, sponsored by the Belgian government.

## References and Notes

(1) Richards, R. E.; Rees, L. V. C. *Langmuir* **1987**, *3*, 335−340.
(2) Millot, B.; Methivier, A.; Jobic H. *J. Phys. Chem. B* **1998**, *102*, 3210−3215.
(3) Sun, M. S.; Talu, O.; Shah, D. B. *J. Phys. Chem.* **1996**, *100*, 17276−17280.
(4) Jasra, R. V.; Choudary, N. V.; Bhat, S. G. T.; Patel, A. G.; Subrahmanyam, N. *Sep. Sci. Technol.* **1997**, *32* (9), 1571−1587.
(5) Dessau, R. M. Adsorption Ion Exchange with Synthetic Zeolites; ACS Symposium Series, 135; American Chemical Society: Washington, D.C., 1980; pp 123−135.
(6) Zhu, W.; van der Graaf, J. M.; van den Broeke, L. J. P.; Kapteijn, F.; Moulijn, J. A. *Ind. Eng. Chem. Res.* **1998**, *37*, 1934−1942.
(7) Yang, Y.; Rees, L. V. C. *Microporous Mater.* **1997**, *12*, 117−122.
(8) Stach, H.; Lohse, U.; Thamm, H.; Schirmer, W. *Zeolites* **1986**, *6*, 74−90.
(9) Zhu, W.; Kapteijn, F.; Moulijn, J. A. *Phys. Chem. Chem. Phys.* **2000**, *2*, 1989−1995.
(10) Jacobs, P. A.; Beyer, H. K.; Valyon, J. *Zeolites* **1981**, *1*, 161−168.
(11) Titiloye, J. O.; Parker, S. C.; Stone, F. S.; Catlow, C. R. A. *J. Phys. Chem.* **1991**, *95*, 4038−4044.
(12) Thamm, H. *Zeolites* **1987**, *7*, 341−346.
(13) Lercher, J. A.; Seshan, K. *Curr. Opin. Solid State Mater. Sci.* **1997**, *2* (1), 57−62.
(14) Smit, B.; Siepmann, J. I. *J. Phys. Chem.* **1994**, *98*, 8442−8452.
(15) Ashtekar, S.; McLeod, A. S.; Mantle, M. D.; Barrie, P. J.; Gladden, L. F. *J. Phys. Chem. B* **2000**, *104*, 5281−5287.
(16) Smit, B.; Maesen, T. L. M. *Nature* **1995**, *374*, 42−44.
(17) Maginn, E. J.; Bell, A. T.; Theodorou, D. N. *J. Phys. Chem.* **1995**, *99*, 2057−2079.
(18) Schenk, M.; Vidal, S. L.; Vlugt, T. J. H.; Smit, B.; Krishna, R. *Langmuir* **2001**, *17*, 1558−1570.
(19) van Well, W. J. M.; Wolthuizen, J. P.; Smit, B.; Van Hooff, J. H. C.; Van Santen, R. A. *Angew. Chem.* **1995**, *107* (22), 2765−2767.
(20) Choudhary, V. R.; Singh, A. P. *Zeolites* **1986**, *6*, 206−208.
(21) Denayer, J. F. M.; De Meyer, K.; Martens, J. A.; Baron, G. V. *Angew. Chem., Int. Ed.* **2003**, *42*, 2774−2777.
(22) Siepmann, J. I.; Martin, M. G.; Mundy, C. J.; Klein, M. L. *Mol. Phys.* **1997**, *90*, 687−693.
(23) Vlugt, T. J. H.; Krishna, R.; Smit, B. *J. Phys. Chem. B* **1999**, *103*, 1102−1118.
(24) Chempath, S.; De Meyer, K. M. A.; Denayer, J. F. M.; Baron, G. V.; Snurr, R. Q. Submitted for publication in *Langmuir*.
(25) Krishna, R.; Calero, S.; Smit, B. *Chem. Eng. J.* **2002**, *88*, 81−94.
(26) Macedonia, M. D.; Maginn, E. J. *Mol. Phys.* **1999**, *96*, 1375−1390.
(27) Du, Z.; Manos, G.; Vlugt, T. J. H.; Smit, B. *AIChE J.* **1998**, *44* (8), 1756−1764.
(28) Krishna, R.; Smit, B.; Calero, S. *Chem. Soc. Rev.* **2002**, *31*, 185−194.
(29) Calero, S.; Smit, B.; Krishna, R. *Phys. Chem. Chem. Phys.* **2001**, *3*, 4390−4398.